

Adaptive Scheduling and Trajectory Design for Power-Constrained Wireless UAV Relays

Matthew Bliss and Nicolò Michelusi

Abstract

This paper investigates the adaptive trajectory and communication scheduling design for an unmanned aerial vehicle (UAV) relaying random data traffic generated by ground nodes to a base station. The goal is to minimize the expected average communication delay to serve requests, subject to an average UAV mobility power constraint. It is shown that the problem can be cast as a semi-Markov decision process with a two-scale structure, which is optimized efficiently: in the outer decision, the UAV radial velocity for *waiting* phases and end radius for *communication* phases optimize the average long-term delay-power trade-off; given outer decisions, inner decisions greedily minimize the instantaneous delay-power cost, yielding the optimal angular velocity in waiting states, and the optimal relay strategy and UAV trajectory in communication states. A constrained particle swarm optimization algorithm is designed to optimize these trajectory problems, demonstrating 100 \times faster computational speeds than successive convex approximation methods. Simulations demonstrate that an intelligent adaptive design exploiting realistic UAV mobility features, such as helicopter translational lift, reduces the average communication delay and UAV mobility power consumption by 44% and 7%, respectively, with respect to an optimal hovering strategy and by 2% and 13%, respectively, with respect to a greedy delay minimization scheme.

Index Terms

UAV communication, rotary-wing UAV, trajectory optimization, particle swarm optimization, energy efficiency

I. INTRODUCTION

Recently, research into unmanned aerial vehicles (UAVs) operating in wireless networks has surged, thanks to their unique advantages over terrestrial base stations (BSs) in terms of mobility,

A preliminary version of this manuscript appeared at IEEE ICC 2020 [1].

Bliss and Michelusi are with the School of Electrical and Computer Engineering, Purdue University, West Lafayette, IN, USA; emails: {blissm,michelus}@purdue.edu.

maneuverability, and enhanced line-of-sight (LoS) link probability [2]–[6]. The potential to exploit UAV mobility for wireless networking applications is vast, and UAVs acting as aerial BSs or relays promise increased cellular coverage, reduced communication delay, and improved energy efficiency [3]. Furthermore, utilizing UAVs not only promises to benefit existing wireless network infrastructure, but to also enable applications still in development, i.e., internet-of-things and public safety applications [3], as well as mobile edge computing and caching [2].

Although demonstrating improvements to wireless networks, designing UAV deployment strategies faces many challenges [2], [3], and trajectory design must consider realistic features of UAV mobility. Already, works such as [7]–[9] included onboard energy constraints, and hence mission times, inherent to many low-altitude platforms [2]. Additionally, UAV path planning presents analytical challenges, due to the large design space, i.e., time-varying UAV and user positions, communication scheduling, channel quality, and quality of service (QoS) constraints [3]. To address these challenges, most prior research on trajectory design focuses on:

- Non-adaptive optimization, i.e., data traffic is known in advance [7], [8], [10], [11];
- Static hovering strategies that incorporate randomness [9], [12]–[19];
- Black-box approaches based on reinforcement learning (RL) [20]–[22].

However, non-adaptive optimization is unrealistic; in practice, wireless networks exhibit random data traffic, which requires adaptive techniques for both the UAV trajectory and communication scheduling. Using static hovering strategies, some works explicitly assume that hovering is energy optimal [18], [19]. However, realistic rotary-wing aircraft features, such as the *helicopter translational lift* phenomenon [23], show that moderate forward flying speeds are more energy-efficient than hovering. Therefore, static hovering deployment has two important drawbacks, namely: 1) it does not fully exploit UAV mobility to improve the channel conditions proactively; 2) it suffers from increased UAV power consumption and reduced endurance. RL-based black-box approaches, on the other hand, fail to leverage the coupling between communication scheduling and UAV trajectory optimization in order to achieve a more efficient design.

To address these open design challenges, in this paper we consider the scenario in which a UAV serves as a relay for randomly generated uplink transmission requests between densely deployed ground nodes (GNs) in a cell and a BS. We formulate an adaptive UAV trajectory and communication scheduling design so as to minimize the expected average communication delay to serve the requests, subject to an average UAV mobility power constraint, and address the following open research challenges, namely: 1) we leverage UAV mobility in order to

simultaneously minimize communication delay and reduce UAV power consumption; 2) we design adaptive schemes capable of adjusting to random data traffic; 3) we leverage the coupling between communication scheduling and UAV trajectory design via a *two-scale decision-making framework*. In contrast to a black-box approach, we demonstrate that the problem can be cast as a semi-Markov decision process (SMDP) and exhibits a two-scale structure that can be optimized efficiently. Numerical simulations reveal that during *waiting* phases in which the UAV is not serving uplink transmission requests, the UAV moves toward an optimized radius so as to fly in a circular path at the power-minimizing speed. Moreover, simulations demonstrate that the intelligent adaptive communication and trajectory design reduces both the average communication delay and UAV mobility power consumption by 44% and 7%, respectively, with respect to an optimal hovering strategy and by 2% and 13%, respectively, with respect to a greedy delay minimization scheme.

A. Related Work

In non-adaptive trajectory design, data traffic is *deterministic* and generated by users before deployment, such that the UAV charts an optimized trajectory and communication schedule before its deployment. For example, [7] designed an energy-efficient trajectory to serve users in fixed positions. In [8], an optimal trajectory was determined so as to minimize the total UAV energy consumption, subject to throughput constraints. However, deterministic data traffic models are impractical in real systems, as transmission requests often arrive randomly and cannot be known in advance. With *random* data traffic, UAV trajectory design and communication scheduling is much more challenging, i.e., both must be continuously adjusted to the outcome of the underlying random processes and consider uncertain changes to the system dynamics.

In fact, adaptive strategies must account for the various realizations that occur due to random data traffic. Even for one realization, the number of possible UAV trajectories to follow is infinite and intractable to optimize without approximation. Likewise, it is not trivial to determine the best relaying strategy, i.e., whether a transmission request transmits directly to its destination or relays through the UAV while following a trajectory. In research, these trajectory optimization problems are often path-discretized [8] and lack convex problem structure. A common approach has been successive convex approximation (SCA), as implemented in [8] and recognized as a standard tool [3], but because previous research neglects random data traffic, only a single SCA-based problem is solved. When many realizations must be solved due to *random* data traffic, the

SCA time consumption prohibits solving all realizations efficiently, as we will show in Sec. VI. In this paper, we develop an alternative heuristic approximation solved with constrained particle swarm optimization (CPSO) which yields comparable accuracy at a fraction of time.

The CPSO meta-heuristic offers attractive convergence rates for complex problems by allowing a population of solutions to explore the search space, combining each individual's best performance, the swarm's best performance, and randomness in updates to avoid convergence to sub-optimal minima [24]. Whereas convex approximation of the objective and constraints changes for each problem (see [7], [8]), CPSO does not depend on the specific problem structure to work effectively. Furthermore, the discretized and approximated data payload constraints, as in [8], can instead be retained as closed-form integrals in the CPSO formulation. Previous UAV communications research has used particle swarm techniques [25]–[30], but either optimized static UAV hovering positions [25]–[29] or imposed a specific structure on the UAV trajectory, e.g., a circular path [30]. In this work, we use CPSO to optimize a series of waypoints and speeds that determine a trajectory, with no other path structures imposed.

Alternatively, works that optimize static UAV hovering positions consider sources of randomness [12]–[14], but are sub-optimal in terms of both UAV endurance [8], [31] and communication performance. For instance, [12] studied optimal UAV placement, showing that user throughput decreased as random user mobility increased, and the UAV was forced to update its position once the throughput fell below a threshold, rather than improve the channel conditions proactively. In our paper, we will show that by intelligently exploiting UAV mobility, i.e., not just hovering in a static position, both the communication performance and UAV power usage can be enhanced.

Works performing RL-based UAV trajectory optimization consider unknown system dynamics, i.e., natural obstructions, user locations, or data traffic [20]–[22]. For example, in [20] a UAV learns the trajectory to maximize a cumulative reward in the presence of random data traffic and ground user positions. Although RL-based schemes are well-suited to handle random system dynamics, formulations often take a black-box approach, in which problem structures, that could be leveraged to reduce state and action spaces and speed up simulations, are largely set aside [20], [32]. Moreover, overlooking problem structure can lead to an inability to adapt to unforeseen conditions. As [20] notes of its own study, it is unknown how changes to initial UAV starting positions would affect the learned trajectory and, by consequence, the network performance.

To address the aforementioned challenges, our previous work [33] investigated the UAV trajectory and communication scheduling design subject to random data traffic from two ground

nodes, but did not consider the UAV mobility power, and assumed the UAV to be the ultimate destination of the GN data traffic. The model was extended in our work [1] to account for the UAV power constraint and the scenario in which the UAV *relays* random data traffic generated by densely deployed GNs and a BS. However, UAV relaying periods utilized a *fly-hover-communicate* strategy, which is inefficient for network performance and UAV endurance, but easier to analyze than protocols in which the UAV communicates while moving [8], as done in this paper.

B. Contributions

- We demonstrate that the optimal trajectory and communication strategy exhibits a two-scale structure that can be efficiently optimized: in the outer decision, the UAV radial velocity for the *waiting* phase and end radius for the *communication* phase are selected to minimize the average long-term delay-power tradeoff; with the outer decisions, the inner decision greedily minimizes the instantaneous delay-power cost, providing the optimal angular velocity in the *waiting* states and optimal relay strategy and UAV trajectory in the *communication* states;
- We develop a value iteration algorithm that leverages sufficient statistics of the system, i.e., only the UAV radius in *waiting* phases and relative UAV-GN positions in *communication* phases, in order to solve the outer decisions as an average cost per stage SMDP;
- We develop a CPSO algorithm to optimize the UAV trajectories of the communication phases in the inner decisions, and show that it performs very competitively to SCA, with computational speeds up to $100\times$ faster.

The remainder of the paper is organized as follows. In Sec II, we introduce the system model; in Sec. III we formulate the optimization goal and formalize the problem as a semi-Markov decision process; in Sec. IV, we present the two-scale optimization approach; in Sec. V, we formulate the trajectory optimization using CPSO; in Sec. VI, we provide the numerical results, followed by concluding remarks in Sec. VII.

II. SYSTEM MODEL

A. Physical Setup

Consider the scenario depicted in Fig 1, where densely deployed ground nodes (GNs) in a circular cell of radius a on the flat ground surface (x - y plane) generate random data traffic to

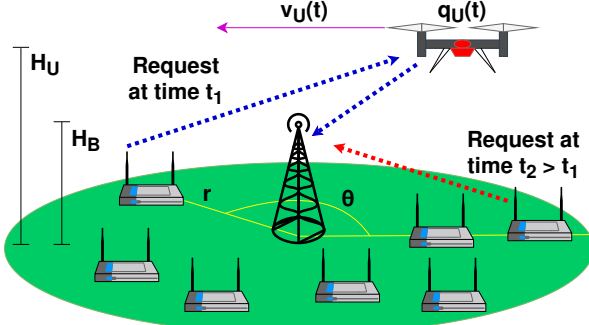


Fig. 1: System model.

be transmitted in the uplink¹ to a base station (BS) located in the center of the cell at height H_B above the ground. The GNs are distributed uniformly in the circular cell with density λ_G [GNs/m²]. Due to poor pathloss conditions experienced by GNs farther away from the BS (e.g., low-power sensors or IoT devices), a rotary-wing UAV is deployed as a mobile relay, flying at a fixed height H_U above the ground: whenever a GN receives a data payload, it either transmits it directly to the BS or relays through the UAV. Let $\mathbf{q}_U(t) = (r_U(t), \theta_U(t)) \in \mathbb{R}_+ \times [0, 2\pi)$ be the polar coordinate of the UAV projected onto the x - y plane, with $r_U(t)$ and $\theta_U(t)$ denoting the UAV's radius and angle with respect to the BS at time t and let $v_U(t)$ be its instantaneous forward flying speed at time t .

B. Communication Model

Each GN generates uplink transmission requests, each with data size L bits, according to a Poisson process with rate λ_P [requests/GN/sec]. Thus overall, uplink transmission requests arrive in time according to a Poisson process with rate $\lambda = \lambda_G \cdot \lambda_P$ [requests/sec/m²]. It follows that the angular coordinate θ of a received transmission request is uniform in $[0, 2\pi]$, and its radial coordinate distribution is $f_R(r) = \frac{2r}{a^2} \mathbb{I}(r \leq a)$, where $\mathbb{I}(\cdot)$ denotes the indicator function.

When an uplink transmission request is received, the GN will either 1) transmit directly to the BS, or 2) relay through the UAV using a two-phase decode-and-forward (DF) protocol (see Sec. III-A), where the UAV, while following a trajectory part of the design, first receives the entire data payload from the GN, and subsequently forwards it to the BS. This decision is made by the BS and is based on the GN position (r, θ) and current UAV position $\mathbf{q}_U(t)$ (so that, for

¹This framework can be extended to an uplink and downlink setting by creating an additional state differentiating the two types of data traffic.

instance, a GN near the BS performs a direct transmission to the BS), and is part of our design, to be formalized. As a result, three distinct communication links must be considered, namely, the GN→BS, GN→UAV, and the UAV→BS links. Assuming that all GNs transmit with a fixed power P_{GN} , the communication rate for the GN→BS link is

$$R_{GB}(r) \triangleq B \log_2 \left(1 + \frac{\gamma_{GB}}{d_{GB}^{\alpha}(r)} \right), \quad (1)$$

where B is the channel bandwidth (Hz), γ_{GB} is the SNR referenced at 1-meter, $d_{GB}(r) = \sqrt{H_B^2 + r^2}$ is the GN-BS distance, and $\alpha \geq 2$ is the pathloss exponent. We assume that the UAV relay phases experience LoS links, which are dominant in low-altitude platforms [5]. Hence, with the UAV in position $\mathbf{q}_U(t) = (r_U(t), \theta_U(t))$, and assuming a fixed UAV transmission power P_{UAV} , the instantaneous communication rates for the GN→UAV and UAV→BS links are

$$R_{GU}(d_{GU}(t)) \triangleq B \log_2 \left(1 + \frac{\gamma_{GU}}{d_{GU}^2(t)} \right), \quad R_{UB}(d_{UB}(t)) \triangleq B \log_2 \left(1 + \frac{\gamma_{UB}}{d_{UB}^2(t)} \right), \quad (2)$$

where γ_{GU} and γ_{UB} are the SNRs of the two links referenced at 1-meter, and $d_{GU}(t)$ and $d_{UB}(t)$ are the GN-UAV and UAV-BS distances at time t .

C. UAV Mobility Power Model

Let $P_U(t) = P_c(t) + P_{\text{mob}}(v_U(t))$ be the instantaneous UAV power consumption, including the total communication power $P_c(t)$ and the forward flight mobility power $P_{\text{mob}}(v_U(t))$, a generally non-convex function of the UAV horizontal flying speed, vehicle drag coefficient, and total weight (e.g., vehicle battery and added equipment) [31]. However, as the communication power (order of 1W) is usually dwarfed by the UAV mobility power (order of 200-1kW [8]), in this paper we neglect the communication power and approximate $P_U(t) \approx P_{\text{mob}}(v_U(t))$.

We use the analytical model for rotary-wing UAVs in forward flight [8],

$$P_{\text{mob}}(V) = P_1 \left(1 + \frac{3V^2}{U_{\text{tip}}^2} \right) + P_2 \left(\sqrt{1 + \frac{V^4}{4v_0^4}} - \frac{V^2}{2v_0^2} \right)^{1/2} + P_3 V^3, \quad (3)$$

where P_1 , P_2 , and P_3 are scaling constants, U_{tip} is the rotor blade tip speed, and v_0 is the mean rotor induced velocity while hovering (see [8] for details). This model is validated by real UAV deployments [31], and an example power vs. speed curve is found in [8], for reference. Therein, hovering requires 1.37kW, whereas flying at the power-minimizing speed of 22m/s only consumes 0.94kW. In the subsequent analysis, we let $P_{\min} = \min_{V \in [0, V_{\max}]} P_{\text{mob}}(V)$ be

the minimum UAV mobility power, and V_{\min} be the power minimizing speed. In fact, in the analysis to follow, we will demonstrate that a nonzero power-minimizing flying speed can be exploited to simultaneously reduce the communication delay and the UAV power consumption, hence improving the UAV endurance.

III. OPTIMIZATION GOAL AND SMDP FORMULATION

In this paper, we design the UAV trajectory and the scheduling decision, so as to minimize the average delay to serve random GN requests, under an average UAV power constraint. At any time, the system is in one of the following phases. In the *waiting phase*, no GN requests are being served by the UAV. When a new GN request arrives, the system transitions to the *request scheduling phase*, where the BS decides if the GN transmits its data payload directly to the BS, or relays through the UAV. Using direct transmission, the system immediately re-enters the *waiting phase*, as the UAV remains free to serve future transmission requests, while the BS directly serves the uplink transmission, with the rate given by (1). Otherwise, the system enters the *UAV relay phase*, where the GN relays its data payload through the UAV using the two-phase DF protocol described in Sec. III-A; after this phase terminates, the system enters the *waiting phase* again. We assume that the UAV can handle only one transmission request at a time, whereas the BS has sufficient capacity to accommodate simultaneous transmissions over orthogonal sub-channels². Thus, new requests received during a *UAV relay phase* are immediately served by direct transmission to the BS.

We define a *decision interval* as the time duration spanning the start of a *waiting phase*, the subsequent *request scheduling phase* when a GN request is received, until the system re-enters the *waiting phase* after scheduling a direct transmission to the BS, or following the *UAV relay phase*. Consider the u th such decision interval; let $\Delta_u^{(w)}$ be the time to wait for a new request, and $\Delta_u^{(s)}$ be the time to serve such request, either through the BS (denoted with the scheduling decision $\xi_u = 0$) or through the UAV ($\xi_u = 1$). Then, the u th decision interval duration is expressed as $\Delta_u = \Delta_u^{(w)} + \xi_u \Delta_u^{(s)}$, since the *waiting phase* follows immediately after scheduling a direct transmission to the BS. Note that we assume the *request scheduling phases* are immediate, i.e., the BS coordinates a scheduling decision instantaneously. Practically, however, this incurs a small delay, which we assume to be negligible.

²Practically, the number of orthogonal sub-channels, k , is finite, so that the BS state can be modeled as a $M/G/k$ queue. We assume that k is large enough so that the probability that more than k requests need to be served simultaneously, i.e., the queue overflows, is small.

We now formulate the average communication delay and UAV mobility power. Let N_u be the number of additional requests received during the UAV relay phase of the u th decision period, $\Delta_{u,i}^{(bs)}$, $i = 1, \dots, N_u$ be the communication delays to serve these requests directly by the BS. Let E_u be the UAV mobility energy expended during the u th decision interval. Let M_t be the total number of decision intervals completed up to time t . Then, we define the expected average communication delay per GN request under a given joint scheduling, communication, and trajectory policy μ (defined later), with the UAV starting from the geometric center $\mathbf{q}_U(0) = (0, 0)$,³ as the total communication delay accrued until time t , over the total number of requests served until time t ; similarly, we define the expected average UAV power as the total energy consumption, over the total duration of the M_t decision intervals up to time t ; mathematically,

$$\bar{D}_\mu \triangleq \lim_{t \rightarrow \infty} \mathbb{E}_\mu \left[\frac{\sum_{u=1}^{M_t} [\Delta_u^{(s)} + \xi_u \sum_{i=1}^{N_u} \Delta_{u,i}^{(bs)}]}{\sum_{u=1}^{M_t} (1 + \xi_u N_u)} \right], \quad \bar{P}_\mu \triangleq \lim_{t \rightarrow \infty} \mathbb{E}_\mu \left[\frac{\sum_{u=1}^{M_t} E_u}{\sum_{u=1}^{M_t} \Delta_u} \right]. \quad (4)$$

Note that \bar{D}_μ in (4) captures all request scenarios, i.e., those relayed through the UAV ($\xi_u = 1$), those transmitted directly to the BS ($\xi_u = 0$), as well as the N_u additional requests served directly by the BS that arrive during the UAV relay phase of the u th decision interval.

To simplify these expressions, let

$$\begin{cases} \bar{E}_\mu \triangleq \lim_{t \rightarrow \infty} \mathbb{E}_\mu \left[\frac{1}{M_t} \sum_{u=1}^{M_t} E_u \right], \\ \bar{T}_\mu \triangleq \lim_{t \rightarrow \infty} \mathbb{E}_\mu \left[\frac{1}{M_t} \sum_{u=1}^{M_t} \Delta_u \right], \\ \bar{N}_\mu \triangleq \lim_{t \rightarrow \infty} \mathbb{E}_\mu \left[\frac{1}{M_t} \sum_{u=1}^{M_t} (1 + \xi_u N_u) \right], \\ \bar{W}_\mu \triangleq \lim_{t \rightarrow \infty} \mathbb{E}_\mu \left[\frac{1}{M_t} \sum_{u=1}^{M_t} [\Delta_u^{(s)} + \xi_u \sum_{i=1}^{N_u} \Delta_{u,i}^{(bs)}] \right], \end{cases} \quad (5)$$

be the expected average UAV energy expenditure, duration, number of requests served, and total communication delays accrued per decision interval, under a policy μ . We can then use Little's Law [34] to express $\bar{P}_\mu = \bar{E}_\mu / \bar{T}_\mu$ and $\bar{D}_\mu = \bar{W}_\mu / \bar{N}_\mu$. With these definitions, we aim to determine the optimal policy μ^* that defines the request scheduling, communication strategy, and UAV trajectory, that solves the power constrained average delay minimization problem⁴

$$\bar{D}_\mu^* = \min_{\mu} \frac{\bar{W}_\mu}{\bar{N}_\mu} \quad \text{s.t.} \quad \frac{\bar{E}_\mu}{\bar{T}_\mu} \leq P_{\text{avg}}. \quad (6)$$

³In the following, expectations $\mathbb{E}_\mu[\cdot]$ will be implicitly assumed to be conditioned on $\mathbf{q}_U(0) = (0, 0)$.

⁴Without loss of generality, we assume $P_{\text{avg}} \geq P_{\text{min}}$, since any $P_{\text{avg}} < P_{\text{min}}$ is not feasible.

Note that this problem is not trivial. In fact, link quality is maximized when the UAV flies at *maximum* speed towards the transmitter (GN in the first phase of the DF protocol, see Sec. III-A) or receiver (BS in the second phase of the DF protocol) and *hovers* on top, but this may violate the average power constraint, because these speeds are not energy-efficient.

Note the inherent complexity that is required to solve \bar{D}_μ^* . As the policy varies, the delay metric changes both the numerator and denominator terms, which cannot be solved with standard dynamic programming algorithms. Equivalently, one can solve the optimization problem⁵

$$\bar{D}_\mu^* = \min_{\mu, n \geq 1} \frac{1}{n} \bar{W}_\mu \text{ s.t. } \bar{E}_\mu - P_{\text{avg}} \bar{T}_\mu \leq 0, \quad n - \bar{N}_\mu \leq 0, \quad (7)$$

by first optimizing μ for fixed $n \geq 1$, and then optimizing $n \geq 1$ via exhaustive search. For a fixed $n \geq 1$, μ can be optimized by solving the Lagrangian problem

$$g_n(\nu) \triangleq \min_{\mu} \frac{1}{n} \bar{W}_\mu + \nu_1 (\bar{E}_\mu - P_{\text{avg}} \bar{T}_\mu) + \nu_2 (n - \bar{N}_\mu), \quad (8)$$

with dual variables $\nu = (\nu_1, \nu_2) \geq 0$, followed by the dual maximization $\nu^* = \max_{\nu \geq 0} g_n(\nu)$, which can be carried out iteratively via projected subgradient ascent [35]. For given n and ν , (8) can be solved using dynamic programming to determine the optimal policy $\mu^{(n, \nu)}$, the dual function $g_n(\nu)$ and subgradients $(\bar{E}_{\mu^{(n, \nu)}} - P_{\text{avg}} \bar{T}_{\mu^{(n, \nu)}})$ and $(n - \bar{N}_{\mu^{(n, \nu)}})$ used to update ν . However, this approach is complex due to the multiple layers of optimization needed: over the policy μ given n, ν ; over $\nu = (\nu_1, \nu_2)$ given n ; and over n . We now propose an alternative optimization criterion with reduced complexity.

Consider the term \bar{W}_μ in (5). If $\xi_u = 1$, then additional requests received during the UAV relay phase are served directly by the BS, with delay $L/R_{GB}(r)$ for a GN in position (r, θ) . Therefore, the expected average communication delay to serve these additional requests is the expected delay with respect to the GN radial distribution,

$$\bar{\Delta}_{BS} \triangleq \mathbb{E}[\Delta_{u,i}^{(bs)}] = \int_0^a \frac{L}{R_{GB}(r)} f_R(r) dr. \quad (9)$$

We can then express \bar{W}_μ as

$$\bar{W}_\mu = \lim_{t \rightarrow \infty} \mathbb{E}_\mu \left[\frac{1}{M_t} \sum_{u=1}^{M_t} [\Delta_u^{(s)} + \xi_u N_u \bar{\Delta}_{BS}] \right] = \bar{\Delta}_{BS} (\bar{N}_\mu - 1) + \bar{W}_\mu^{(s)}, \quad (10)$$

⁵For fixed policy μ , the optimization over $n \geq 1$ yields $n = \bar{N}_\mu$ so that (6) and (7) are equivalent.

where the second step uses the definition of \bar{N}_μ in (5), and we have defined the expected delay of the requests for which a scheduling decision has been made (opposed to those served directly by the BS during the *UAV relay phase*) as

$$\bar{W}_\mu^{(s)} \triangleq \lim_{t \rightarrow \infty} \mathbb{E}_\mu \left[\frac{1}{M_t} \sum_{u=1}^{M_t} \Delta_u^{(s)} \right]. \quad (11)$$

Then, with $\bar{N}_\mu \geq 1$, we can express the average delay as

$$\bar{D}_\mu = \frac{\bar{W}_\mu}{\bar{N}_\mu} = \frac{1}{\bar{N}_\mu} \bar{W}_\mu^{(s)} + \left(1 - \frac{1}{\bar{N}_\mu}\right) \bar{\Delta}_{BS}. \quad (12)$$

Next, we show that \bar{D}_μ can be upper and lower bounded. Let μ_{BS} be the policy such that the UAV flies at the power-minimizing speed V_{\min} , and all requests are served by the BS. This policy is feasible (it uses minimum power) and its average delay is $\bar{D}_{\mu_{BS}} = \bar{\Delta}_{BS}$, since all requests are served directly by the BS. Therefore, under the optimal policy we must have $\bar{D}_\mu^* \leq \bar{D}_{\mu_{BS}} = \bar{\Delta}_{BS}$. Using (12) and the fact that $\bar{N}_\mu \geq 1$, this implies that $\bar{W}_{\mu^*}^{(s)} \leq \bar{\Delta}_{BS}$. Let μ be any policy that satisfies $\bar{W}_\mu^{(s)} \leq \bar{\Delta}_{BS}$ (note that any other policy is suboptimal). Under such policy, (12) along with $\bar{N}_\mu \geq 1$, implies $\bar{W}_\mu^{(s)} \leq \bar{D}_\mu \leq \bar{\Delta}_{BS}$.

Moreover, if $\xi_u = 1$, then N_u requests are received during the *UAV relay phase* of duration $\Delta_u^{(s)}$; since these requests are received with an overall rate $\Lambda \triangleq \lambda\pi a^2$, we find that $\mathbb{E}[N_u | \Delta_u^{(s)}] = \Delta_u^{(s)} \Lambda$, so that using the bound $\xi_u \leq 1$, we can express

$$\bar{N}_\mu = \lim_{t \rightarrow \infty} \mathbb{E}_\mu \left[\frac{1}{M_t} \sum_{u=1}^{M_t} [1 + \xi_u \Delta_u^{(s)} \Lambda] \right] \leq 1 + \Lambda \bar{W}_\mu^{(s)}, \quad (13)$$

with strict equality if the UAV always serves requests. Under any policy μ such that $\bar{W}_\mu^{(s)} \leq \bar{\Delta}_{BS}$, we can then bound

$$\bar{W}_\mu^{(s)} \leq \bar{D}_\mu \leq \bar{J}_\mu^{(s)} \triangleq \bar{W}_\mu^{(s)} \frac{1 + \Lambda \bar{\Delta}_{BS}}{1 + \Lambda \bar{W}_\mu^{(s)}} \leq \bar{\Delta}_{BS}, \quad (14)$$

where the second inequality follows from $\bar{W}_\mu^{(s)} \leq \bar{\Delta}_{BS}$. Remarkably, the lower and upper bounds of \bar{D}_μ , given by $\bar{W}_\mu^{(s)}$ and $\bar{J}_\mu^{(s)}$, respectively, are both increasing functions of $\bar{W}_\mu^{(s)}$. This observation motivates us to look at the alternative optimization problem

$$\min_{\mu} \bar{W}_\mu^{(s)} \text{ s.t. } \bar{E}_\mu - P_{\text{avg}} \bar{T}_\mu \leq 0, \quad (15)$$

which optimizes both upper and lower bounds to the optimal delay, as shown in (14). This prob-

lem will be the focus of the following analysis. To solve it, we use the Lagrangian formulation

$$\begin{aligned} g(\nu) &= \min_{\mu} \left(\bar{W}_{\mu}^{(s)} + \nu(\bar{E}_{\mu} - P_{\text{avg}}\bar{T}_{\mu}) \right) \\ &= \min_{\mu} \lim_{t \rightarrow \infty} \mathbb{E}_{\mu} \left[\frac{1}{M_t} \sum_{u=1}^{M_t} (\Delta_u^{(s)} + \nu(E_u - P_{\text{avg}}\Delta_u)) \right] \end{aligned} \quad (16)$$

where ν is the dual variable, optimized by maximizing $\max_{\nu \geq 0} g(\nu)$. In the next section, we demonstrate that for a given $\nu \geq 0$, (16) can be cast as a semi-Markov decision process (SMDP) and solved with dynamic programming tools. Note the advantage of the problem (16) with respect to the problem (8). To solve (8) would require optimizing over twice as many dual variables and an exhaustive search over the value n , whereas the dual maximization of (16) is done only with respect to a single dual variable ν .

A. SMDP Formulation

In this section, we formulate the problem (16) as a SMDP. We first characterize the states, actions, and policy of this SMDP, and then optimize via dynamic programming tools. In general, the state at any time requires knowledge of the UAV position, whether or not there is an active request for uplink transmission, and if there is, the location of the requesting GN. Let $\mathcal{Q}_{\text{UAV}} \triangleq \mathbb{R}_+ \times [0, 2\pi)$ define the set of UAV positions, and $\mathcal{Q}_{\text{GN}} \triangleq [0, a] \times [0, 2\pi)$ the set of possible GN request positions, both expressed as polar coordinates. The general state space, \mathcal{S} , can be defined by a partition of two-subsets, namely, the *waiting states* $\mathcal{S}_{\text{wait}} = \mathcal{Q}_{\text{UAV}} \times \{w_0\}$ and the *communication states* $\mathcal{S}_{\text{comm}} = \mathcal{Q}_{\text{UAV}} \times \mathcal{Q}_{\text{GN}}$, where the point $w_0 \triangleq (-1, -1)$ denotes the case in which there is no active transmission request.

Note that although the *scheduling* and *UAV relay* phases are defined separately in the problem formulation, Sec. III, this is a purely logical distinction to describe the sequence of decisions to be made. In this section, we combine these two phases into a single *communication scheduling and trajectory selection* action, which comprises: 1) the scheduling decision $\xi \in \{0, 1\}$, which determines if the request is served directly by the BS ($\xi = 0$) or relayed through the UAV ($\xi = 1$); and 2) if $\xi = 1$, the trajectory strategy of the UAV.

Key to the definition of the SMDP is how the system is sampled in time so as to define Markovian dynamics in the evolution of the sampled states. To this end, we sample the continuous time interval to define a sequence of states $\{s_n, n \geq 0\} \subseteq \mathcal{S}$ with the Markov property, as specified below. Along with it, we define the actions available in each state, the transition probabilities,

as well as the duration $T(s, \mathbf{a})$, UAV energy expenditure $E(s, \mathbf{a})$, and communication delay cost $\Delta(s, \mathbf{a})$ metrics accrued in state s under action \mathbf{a} .

If the UAV is in the *waiting state* state $s_n = (\mathbf{q}_U(t), w_0) \in \mathcal{S}_{\text{wait}}$ at time t , i.e., it is in the continuous-space position $\mathbf{q}_U(t)$ and there are no active requests, then the actions available are to move the UAV (parallel to the x - y plane) with radial and angular velocity components (v_r, θ_c) , over an arbitrarily small duration $\Delta_0 \ll 1/\Lambda$. Note that the angular velocity component, θ_c , is perpendicular to the UAV position vector and points counter-clockwise, and the radial velocity is referred to the outward direction. Under a maximum speed constraint V_{\max} , the action space in the *waiting state* (r_U, θ_U, w_0) is then defined as

$$\mathcal{A}_{\text{wait}}(r_U) \triangleq \left\{ (v_r, \theta_c) \in \mathbb{R}^2 \mid \sqrt{v_r^2 + r_U^2 \cdot \theta_c^2} \leq V_{\max} \right\}, \quad (17)$$

which solely depends on the radial state r_U , where $\sqrt{v_r^2 + r_U^2 \cdot \theta_c^2}$ is the speed expressed with respect to polar coordinates. In state $s = (r_U, \theta_U, w_0) \in \mathcal{S}_{\text{wait}}$, under action $\mathbf{a} = (v_r, \theta_c) \in \mathcal{A}_{\text{wait}}(r_U)$, the cost metrics are given by

$$\Delta(s; \mathbf{a}) = 0, \quad E(s; \mathbf{a}) = \Delta_0 P_{\text{mob}} \left(\sqrt{v_r^2 + r_U^2 \cdot \theta_c^2} \right), \quad T(s; \mathbf{a}) = \Delta_0. \quad (18)$$

In fact, the communication delay during the *waiting phase* is zero, since there is no ongoing communication; the duration of a waiting state visit is Δ_0 , during which the UAV uses an amount of energy $\Delta_0 P_{\text{mob}}(v_U)$ for its mobility, where $v_U = \sqrt{v_r^2 + r_U^2 \cdot \theta_c^2}$ is the UAV speed.

The new state is then sampled at time $t + \Delta_0$. At this time, the new position of the UAV is

$$\mathbf{q}_U(t + \Delta_0) \approx (r_U, \theta_U) + (v_r, \theta_c) \Delta_0. \quad (19)$$

Note that no new request is received in the time interval $[t, t + \Delta_0]$ with probability $e^{-\Lambda \Delta_0}$, so that the new state is a waiting state. Otherwise, a new request is received from a GN in position (r, θ) according to the uniform circular pdf with the radial coordinate distribution $f_R(r)$, so that the new state enters the scheduling and communication phase. Thus, the transition probability from the waiting state $s_n = (\mathbf{q}_U(t), w_0)$ under action $\mathbf{a}_n = (v_r, \theta_c) \in \mathcal{A}_{\text{wait}}(r_U)$ is expressed as

$$\mathbb{P}(s_{n+1} = (r_U + v_r \Delta_0, \theta_U + \theta_c \Delta_0, w_0) \mid s_n = (r_U, \theta_U, w_0), \mathbf{a}_n = (v_r, \theta_c)) = e^{-\Lambda \Delta_0}, \quad (20)$$

$$\mathbb{P}(s_{n+1} \in (\mathbf{q}_U(t + \Delta_0), \mathcal{F}) \mid s_n, \mathbf{a}_n) = [A(\mathcal{F}) \cdot (1 - e^{-\Lambda \Delta_0})] / \pi a^2, \quad \forall \mathcal{F} \subseteq \mathcal{Q}_{\text{GN}}, \quad (21)$$

where $A(\mathcal{F})$ is the area of region \mathcal{F} on the x - y plane. If a request is received in the Δ_0 time

interval, the probability of receiving it from region \mathcal{F} within the cell is given by the area $A(\mathcal{F})$ divided by the cell area, πa^2 , because request locations are uniformly distributed in the cell.

Upon reaching a communication state $s_n = (r_U, \theta_U, r, \theta) \in \mathcal{S}_{\text{comm}}$ at time t , the system must serve a GN request at position (r, θ) . The BS first determines the scheduling decision $\xi \in \{0, 1\}$:

- 1) When $\xi = 0$, the GN transmits directly to the BS. The next state is sampled immediately after the decision, at time t . Since this action duration is 0, no new requests are received, so that the new state becomes the waiting state $s_{n+1} = (r_U, \theta_U, w_0) \in \mathcal{S}_{\text{wait}}$ with probability 1.
- 2) When $\xi = 1$, the UAV can choose any feasible trajectory starting from the current position $\mathbf{q}_U(t) = (r_U, \theta_U)$ which allows the GN to transmit the entire data payload of L bits to the BS, by *relaying* through the UAV. This mechanism is described next.

When the UAV is chosen to relay the data payload, let \mathbf{q}_U be the trajectory selected. The communication then follows a two-phase DF approach: in the first phase, of duration t_p , the GN transmits its payload to the UAV; in the second phase, of duration $\Delta - t_p$, the UAV relays the data payload to the BS. Assuming a *move-and-transmit* strategy (see [8]), the trajectory and durations t_p and $\Delta - t_p$ of the two phases must satisfy

$$\int_0^{t_p} R_{GU}(d_{GU}(t + \eta))d\eta \geq L, \quad \int_{t_p}^{\Delta} R_{UB}(d_{UB}(t + \eta))d\eta \geq L, \quad (\text{C.1})$$

i.e., the entire payload is transmitted to the UAV and then to the BS, so that the total communication delay of the two-phase DF scheme is Δ . We define the action space in state $(r_U, \theta_U, r, \theta) \in \mathcal{S}_{\text{comm}}$, when $\xi = 1$, as the set of feasible trajectories following the two-phase DF communication approach, that start in position (r_U, θ_U) , with the GN located in position (r, θ) , in which the UAV serves as a relay. This set is defined as $\mathcal{T}_{r,\theta}(r_U, \theta_U) \triangleq \bigcup_{\hat{\theta}_U \in [0, 2\pi)} \bigcup_{\hat{r}_U \in \mathbb{R}_+} \mathcal{T}_{r,\theta}(r_U, \theta_U \rightarrow \hat{r}_U, \hat{\theta}_U)$, where $\mathcal{T}_{r,\theta}(r_U, \theta_U \rightarrow \hat{r}_U, \hat{\theta}_U)$ is the set of feasible UAV trajectories starting in position (r_U, θ_U) , terminating in position $(\hat{r}_U, \hat{\theta}_U)$, and serving a GN located at (r, θ) via the DF protocol, i.e.,

$$\begin{aligned} \mathcal{T}_{r,\theta}(r_U, \theta_U \rightarrow \hat{r}_U, \hat{\theta}_U) = \Big\{ & \mathbf{q}_U : [0, \Delta] \mapsto \mathbb{R}_+ \times [0, 2\pi) : \text{C.1}, \\ & v_U(\eta) \leq V_{\max}, \quad \forall \eta \in [0, \Delta], \end{aligned} \quad (\text{C.2})$$

$$\mathbf{q}_U(0) = (r_U, \theta_U), \quad \mathbf{q}_U(\Delta) = (\hat{r}_U, \hat{\theta}_U), \quad \exists \Delta \geq 0, \exists 0 \leq t_p \leq \Delta \Big\}; \quad (\text{C.3})$$

in this definition, C.1 reflects the data payload constraints, C.2 the maximum speed constraint, and C.3 the trajectory constraints. The total action space of the *communication states* $s = (r_U, \theta_U, r, \theta) \in \mathcal{S}_{\text{comm}}$ is thus defined by $\mathcal{A}_{\text{comm}}(r_U, \theta_U, r, \theta) \triangleq \{0\} \cup \mathcal{A}_{\text{traj}}(r_U, \theta_U, r, \theta)$, where

the point $\{0\}$ reflects the option $\xi = 0$, i.e., the GN transmits directly to the BS, and

$$\mathcal{A}_{\text{traj}}(r_U, \theta_U, r, \theta) \triangleq \{(\hat{r}_U, \hat{\theta}_U, \mathbf{q}_U) : (\hat{r}_U, \hat{\theta}_U) \in \mathcal{Q}_{\text{GN}}, \mathbf{q}_U \in \mathcal{T}_{r, \theta}(r_U, \theta_U \rightarrow \hat{r}_U, \hat{\theta}_U)\} \quad (22)$$

is the set of feasible trajectories that can be taken when the UAV is selected to relay ($\xi = 1$).

For the delay, energy, and time metrics of the *communication* states $s = (r_U, \theta_U, r, \theta) \in \mathcal{S}_{\text{comm}}$, there are two cases. First, when $\xi = 0$ (direct transmission) is selected,

$$\Delta(s; 0) = \frac{L}{R_{GB}(r)}, \quad E(s; 0) = 0, \quad T(s; 0) = 0, \quad (23)$$

where $R_{GB}(r)$ is the communication rate for the direct transmission defined in (1), and the other two terms equal 0 since the system moves immediately to the waiting state $(r_U, \theta_U, w_0) \in \mathcal{S}_{\text{wait}}$ with probability 1, and the corresponding action duration and energy consumption are 0.

Instead, when the UAV is chosen for relaying ($\xi = 1$), and an action $\mathbf{a} = (\hat{r}_U, \hat{\theta}_U, \mathbf{q}_U)$ is taken, the metrics are

$$\Delta(s; \mathbf{a}) = \Delta, \quad E(s; \mathbf{a}) = \int_0^\Delta P_{\text{mob}}(v_U(\eta)) d\eta, \quad T(s; \mathbf{a}) = \Delta, \quad (24)$$

where Δ is the duration of the selected trajectory \mathbf{q}_U . In fact, the communication delay incurred during this *communication* phase is Δ , which is also the duration of this *communication* state visit, and the energy is the integration of the UAV mobility power over the trajectory.

Upon completing the *communication* phase when the UAV relays data, the UAV enters the *waiting phase* again; the new state is then sampled at time $t + \Delta$, and is given by $s_{n+1} = (\hat{r}_U, \hat{\theta}_U, w_0) \in \mathcal{S}_{\text{wait}}$. Thus under action $\mathbf{q}_U \in \mathcal{T}_{r, \theta}(r_U, \theta_U \rightarrow \hat{r}_U, \hat{\theta}_U)$, the state transitions from $s_n = (r_U, \theta_U, r, \theta)$ to $s_{n+1} = (\hat{r}_U, \hat{\theta}_U, w_0)$ with probability 1.

Next, we can define a policy μ . For *waiting* states $(r_U, \theta_U, w_0) \in \mathcal{S}_{\text{wait}}$, the policy selects a velocity (v_r, θ_c) from the action space defined in (17), i.e., $\mu(r_U, \theta_U, w_0) \in \mathcal{A}_{\text{wait}}(r_U)$. Likewise, for *communication* states $(r_U, \theta_U, r, \theta) \in \mathcal{S}_{\text{comm}}$, the policy selects the scheduling decision $\xi \in \{0, 1\}$ and, if $\xi = 1$, the trajectory followed in the two-phase DF protocol,

$$\mu(r_U, \theta_U, r, \theta) \in \mathcal{A}_{\text{comm}}(r_U, \theta_U, r, \theta) \triangleq \{0\} \cup \mathcal{A}_{\text{traj}}(r_U, \theta_U, r, \theta). \quad (25)$$

With a *stationary policy* μ defined, the Lagrangian term $L_\mu^{(\nu)} \triangleq \bar{W}_\mu^{(s)} + \nu(\bar{E}_\mu - P_{\text{avg}}\bar{T}_\mu)$ in

(16) in the context of the SMDP is reformulated as

$$L_\mu^{(\nu)} = \lim_{K \rightarrow \infty} \mathbb{E} \left[\frac{\frac{1}{K} \sum_{n=0}^{K-1} \ell_\nu(s_n; \mu(s_n))}{\frac{1}{K} \sum_{n=0}^{K-1} \mathbb{I}(s_n \in \mathcal{S}_{\text{comm}})} \middle| s_0 \right], \quad (26)$$

where $s_0 = (0, 0, w_0)$ (the UAV begins at the cell center with no transmission requests), and the overall Lagrangian metric in state s under action \mathbf{a} is defined as

$$\ell_\nu(s; \mathbf{a}) \triangleq \Delta(s; \mathbf{a}) + \nu(E(s; \mathbf{a}) - P_{\text{avg}} T(s; \mathbf{a})). \quad (27)$$

By specializing this metric for waiting states, using (27), we obtain

$$\ell_\nu(r_U, \theta_U, w_0; v_r, \theta_c) = \nu \left(P_{\text{mob}} \left(\sqrt{v_r^2 + r_U^2 \cdot \theta_c^2} \right) - P_{\text{avg}} \right) \Delta_0; \quad (28)$$

for *communication* states under action $\xi = 0$, we use (23) to obtain $\ell_\nu(r_U, \theta_U, r, \theta; 0) = L/R_{GB}(r)$; for *communication* state action $\xi = 1$ with feasible trajectory \mathbf{q}_U ending in $(\hat{r}_U, \hat{\theta}_U)$, we obtain

$$\ell_\nu(r_U, \theta_U, r, \theta; \hat{r}_U, \hat{\theta}_U, \mathbf{q}_U) \triangleq (1 - \nu P_{\text{avg}}) \Delta + \nu \int_0^\Delta P_{\text{mob}}(v_U(\eta)) d\eta. \quad (29)$$

Using Little's Law [34], we rewrite $L_\mu^{(\nu)}$ in terms of the SMDP steady-state probabilities as

$$L_\mu^{(\nu)} = \frac{\int_{\mathcal{S}} \Pi_\mu(s) \ell_\nu(s; \mu(s)) ds}{\int_{\mathcal{S}_{\text{comm}}} \Pi_\mu(s) ds}, \quad (30)$$

where $\Pi_\mu(s)$ is the steady-state pdf of the system being in a state s under policy μ . However, (30) cannot be solved via standard dynamic programming techniques, due to the dependence of the denominator on the policy μ . Lemma 1 demonstrates that this term can be expressed as a positive constant, *independent* from policy μ , and only dependent on system parameters. In doing so, the optimization of μ only needs to focus on the minimization of $\int_{\mathcal{S}} \Pi_\mu(s) \ell_\nu(s; \mu(s)) ds$, so that the minimization of (30) can be cast as an *average cost per stage problem*, solvable through standard dynamic programming approaches, after discretization of the state space.

Lemma 1. *Let $\pi_{\text{comm}} = \int_{\mathcal{S}_{\text{comm}}} \Pi_\mu(s) ds$ and $\pi_{\text{wait}} = 1 - \pi_{\text{comm}}$ be the steady-state probabilities that the UAV is in the waiting and communication phases in the SMDP, respectively. We have that*

$$\pi_{\text{wait}} = \frac{1}{2 - e^{-\Lambda \Delta_0}}, \quad \pi_{\text{comm}} = \frac{1 - e^{-\Lambda \Delta_0}}{2 - e^{-\Lambda \Delta_0}}. \quad (31)$$

Proof. Let p_{ww} , p_{wc} , p_{cw} , and p_{cc} be the probabilities of remaining in the waiting phase (*ww*), moving from a waiting state to a communication state (*wc*), from a communication to a waiting

state (*cw*), or remaining in the communication phase (*cc*), in one SMDP state transition. Then, $p_{ww} = e^{-\Lambda\Delta_0}$ (if no request is received, the SMDP remains in the waiting state), $p_{wc} = 1 - p_{ww}$, $p_{cw} = 1$, and $p_{cc} = 0$ (if the SMDP is in the communication state, the next state will be a waiting state). Therefore, the steady-state probabilities of the SMDP being in the waiting and communication states, π_{wait} and π_{comm} , satisfy

$$\begin{cases} \pi_{\text{wait}} = p_{ww}\pi_{\text{wait}} + p_{cw}\pi_{\text{comm}} = e^{-\Lambda\Delta_0}\pi_{\text{wait}} + \pi_{\text{comm}}, \\ \pi_{\text{comm}} = p_{wc}\pi_{\text{wait}} + p_{cc}\pi_{\text{comm}} = (1 - e^{-\Lambda\Delta_0})\pi_{\text{wait}}, \\ \pi_{\text{wait}} + \pi_{\text{comm}} = 1, \end{cases}$$

whose solution is given in the statement of the lemma. ■

With the simplification of $\int_{\mathcal{S}_{\text{comm}}} \Pi_\mu(s)ds$ into a positive constant, π_{comm} , the minimization problem of (16) can be expressed as

$$g(\nu) = \frac{1}{\pi_{\text{comm}}} \min_{\mu} \int_{\mathcal{S}} \Pi_\mu(s) \ell_\nu(s; \mu(s)) ds, \quad (32)$$

with the dual maximization $\max_{\nu \geq 0} g(\nu)$. Note that the transition probabilities in Lemma 1 are policy-independent, allowing for the simplification of the denominator.

IV. STATE SPACE SIMPLIFICATION AND TWO-SCALE DECOMPOSITION OF POLICY μ

Because GN transmission requests are distributed uniformly in the circular cell, and the BS is in the cell center, we can reduce the state dimension. Namely, the UAV radius information is a sufficient statistic in decision making for a *waiting* state (r_U, θ_U, w_0) , and thus we can express waiting states as $s = (r_U, w_0) \in \mathcal{S}_{\text{wait}}$. Likewise, for the *communication* states $(r_U, \theta_U, r, \theta)$, only the UAV radius, GN request radius, and the angle *between* them must be known to uniquely characterize the state. Thus *communication* states can be redescribed as $s = (r_U, r, \psi) \in \mathcal{S}_{\text{comm}}$, where $\psi \in [0, 2\pi)$ is the angle between the GN and the current UAV position. A consequence of these sufficient statistics for decision making is that the steady-state probability of the SMDP is only a function of certain action components, namely: the radial velocity v_r and end radius position \hat{r}_U for *waiting* and *communication* states, respectively. Thus, the steady-state probabilities are independent of the angular velocity θ_c and the end angular position $\hat{\theta}_U$ and specific trajectory \mathbf{q}_U of the *waiting* and *communication* states, respectively.

With this observation, let $O(s) \triangleq v_r \in [-V_{\max}, V_{\max}]$ define the *radial velocity policy* of the *waiting* states $s \in \mathcal{S}_{\text{wait}}$, specifying the radial velocity component of a waiting action $\mathbf{a} = (v_r, \theta_c) \in \mathcal{A}_{\text{wait}}(r_U)$; let $U(s) \triangleq \hat{r}_U \in [0, a]$ define the *next radius position policy* of the *communication* states $s \in \mathcal{S}_{\text{comm}}$, specifying the end radius position of a scheduling and communication action $\mathbf{a} \in \mathcal{A}_{\text{comm}}(s)$. In particular, in state $s = (r_U, r, \theta)$ under action $\xi = 0$ (direct transmission to the BS), $U(s) = r_U$ since the system moves immediately to a waiting position with the UAV at distance r_U from the center; on the other hand, under action $\mathbf{a} = (\hat{r}_U, \hat{\theta}_U, \mathbf{q}_U(\cdot))$ (UAV selected as relay, with trajectory \mathbf{q}_U ending in $\hat{r}_U, \hat{\theta}_U$), $U(s) = \hat{r}_U$. Under this decomposition, O and U constitute the policy decisions made by the SMDP and are the only actions to affect the steady-state distribution Π_μ ; thus O and U are defined as *outer decisions*, and we let $\Pi_{O,U}$ be the steady-state distribution of the SMDP under (O, U) . Thus, the optimization problem (32) can be restated as

$$g(\nu) = \frac{1}{\pi_{\text{comm}}} \min_{O,U} \left[\int_{\mathcal{S}_{\text{wait}}} \Pi_{O,U}(s) \ell_\nu^*(s; O(s)) ds + \int_{\mathcal{S}_{\text{comm}}} \Pi_{O,U}(s) \ell_\nu^*(s; U(s)) ds \right], \quad (33)$$

where ℓ_ν^* are *inner decisions*, i.e., the Lagrangian metrics optimized with respect to the action components not specified by O and U . In particular, for waiting states $s = (r_U, w_0)$ and radial velocity $O(s) = v_r$, the inner optimization is

$$\ell_\nu^*(s; O(s)) = \min_{\theta_c} \nu \left(P_{\text{mob}} \left(\sqrt{v_r^2 + r_U^2 \cdot \theta_c^2} \right) - P_{\text{avg}} \right) \Delta_0 \quad \text{s.t.} \quad \sqrt{v_r^2 + r_U^2 \cdot \theta_c^2} \leq V_{\max}. \quad (34)$$

Because $\nu \geq 0$, $\Delta_0 > 0$, and P_{avg} are constant, θ_c^* is the angular velocity minimizing the UAV power consumption for a given UAV radial velocity v_r and radius r_U , solvable through exhaustive search. For communication states $s = (r_U, r, \psi)$, $\ell_\nu^*(s; U(s))$ is determined by optimizing over the scheduling decision $\xi \in \{0, 1\}$ (note that $\xi = 1$ if $U(s) \neq r_U$) and, if $\xi = 1$, the trajectory \mathbf{q}_U followed by the UAV, terminating at the radial position $\hat{r}_U = U(s)$. To formalize it, let $\ell_\nu^*(s; U(s), \xi)$ denote the optimized metric as a function of $\xi \in \{0, 1\}$. For $\xi = 1$,

$$\ell_\nu^*(s; U(s), 1) = \min_{\Delta, \mathbf{q}_U, t_p} (1 - \nu P_{\text{avg}}) \Delta + \nu \int_0^\Delta P_{\text{mob}} \left(\sqrt{r'_U(\eta)^2 + r_U^2(\eta) \cdot \theta'_U(\eta)^2} \right) d\eta \quad (35)$$

$$\text{s.t. C.1, C.2, } \mathbf{q}_U(0) = (r_U, 0), \|\mathbf{q}_U(\Delta)\|_2 = \hat{r}_U, \quad (36)$$

where C.1 reflect the data payload constraints of the two-phase DF protocol, C.2 is the maximum UAV speed constraint, and (36) gives the UAV trajectory starting position and end radius. For

Algorithm 1 Dynamic Programming and Projected Subgradient Ascent Algorithm

1: **init:** $k=0$; dual variable $\nu_0 \geq 0$; step-size $\{\rho_k = \rho_0/(k+1), k \geq 0\}$.
 2: Determine the minimizers, θ_c^* of $\ell_{\nu_k}^*(s; v_r)$, for all $s \in \mathcal{S}_{\text{wait}}$ and *radial velocities* $v_r \in [-V_{\max}, V_{\max}]$.
 3: **for** $k = 0, 1, \dots$ **do**
 4: Calculate $\ell_{\nu_k}^*(s; O(s))$ using ν_k for all $s \in \mathcal{S}_{\text{wait}}$ and $O(s)$ using the values θ_c^* determined.
 5: Calculate $\ell_{\nu_k}^*(s; U(s))$ for all $s \in \mathcal{S}_{\text{comm}}$ and *next radius positions* $U(s) \in [0, a]$, using the CPSO meta-heuristic to be described in Sec. V (Alg. 3).
 6: Determine the optimal policy $\tilde{\mu}_k \triangleq (O_k^*, U_k^*) = \text{VITER}(\nu_k)$ using the value iteration method shown in Alg. 2.
 7: **if** $|g(\nu_k) - g(\nu_{k-1})| < \epsilon_{DI}$; $\bar{E}_{\tilde{\mu}_k} - P_{\text{avg}} \bar{T}_{\tilde{\mu}_k} < \epsilon_{PF}$; $\nu_k |\bar{E}_{\tilde{\mu}_k} - P_{\text{avg}} \bar{T}_{\tilde{\mu}_k}| < \epsilon_{CS}$ **then**
 8: **return:** $\tilde{\mu}_k = (O_k^*, U_k^*)$;
 9: **else**
 10: Update $\nu_{k+1} = [\nu_k + \rho_k \cdot (\bar{E}_{\tilde{\mu}_k} - P_{\text{avg}} \bar{T}_{\tilde{\mu}_k})]^+$, where $[x]^+$ is the projection onto $x \geq 0$;
 11: update $k \leftarrow k + 1$.
 12: **end if**
 13: **end for**

$\xi = 0$ (hence $U(s) = r_U$), using (23) we obtain $\ell_{\nu}^*(s; U(s), 0) = L/R_{GB}(r)$, hence $\ell_{\nu}^*(s; r_U)$ is obtained by further minimizing over the scheduling decision $\xi \in \{0, 1\}$, yielding

$$\ell_{\nu}^*(s; U(s)) = \begin{cases} \min_{\xi \in \{0, 1\}} \ell_{\nu}^*(s; U(s), \xi), & U(s) = r_U \\ \ell_{\nu}^*(s; U(s), 1) & U(s) \neq r_U. \end{cases} \quad (37)$$

Thus, if the outer decision selects $U(s) = r_U$, the inner scheduling decision $\xi \in \{0, 1\}$ is obtained by greedily minimizing a cost metric that trades off communication delay and energy consumption, so that, if $\ell_{\nu}^*(s; U(s), 0) < \ell_{\nu}^*(s; U(s), 1)$, then the transmission is scheduled directly to the BS. Otherwise, $\xi = 1$ is selected, the UAV is used as a relay, and the inner decision trajectory of the UAV greedily minimizes the delay-energy tradeoff, subject to terminating at the target radius of the outer decision $U(s) = \hat{r}_U$.

Note, the problem (35) must consider the dual variable ν and is infinite-dimensional, which entails that some degree of approximation must be used, i.e., discretizing the path into a finite number of straight line segments, with each line segment traversed by the UAV at a constant speed [8]. In Sec. V, we will describe a heuristic approximation of the problem and evaluate its performance in the numerical results of Sec. VI. We now prescribe Alg. 1, highlighting the overall process for solving (33) and its dual maximization with projected subgradient ascent (see [35]). The *outer decision*, i.e., the selection of the radial velocities (O) and next radius positions

Algorithm 2 Value Iteration: $\tilde{\mu} \triangleq (O^*, U^*) = \text{VITER}(\nu)$

```

1: init:  $i=0$ , the value function  $V_i(s)=0$  for all states  $s \in \mathcal{S}$ , and stopping criterion  $\delta$ .
2: repeat
3:   for each  $s = (r_U, w_0) \in \mathcal{S}_{\text{wait}}$  do
4:      $V_{i+1}(s) \leftarrow \min_{v_r \in [-V_{\max}, V_{\max}]} [\ell_{\nu}^*(s; v_r) + e^{-\Lambda\Delta_0} \cdot V_i(r_U + v_r \cdot \Delta_0, w_0)$ 
       $+ (1 - e^{-\Lambda\Delta_0}) \cdot \int_0^{2\pi} \frac{1}{2\pi} \int_0^a \frac{2r'}{a^2} \cdot V_i(r_U + v_r \cdot \Delta_0, r', \psi') dr' d\psi']$  and  $O_{i+1}(s)$  is the arg min.
5:   end for
6:   for each  $s = (r_U, r, \psi) \in \mathcal{S}_{\text{comm}}$  do
7:      $V_{i+1}(s) \leftarrow \min_{\hat{r}_U \in [0, a]} [\ell_{\nu}^*(s; \hat{r}_U) + V_i(\hat{r}_U, w_0)]$  and  $U_{i+1}(s)$  is the arg min.
8:   end for
9:    $\forall s$ , calculate the stopping criteria metric  $H(s) = V_{i+1}(s) - V_i(s)$ .
10:   $i \leftarrow i + 1$ .
11: until  $\max_{s \in \mathcal{S}} H(s) - \min_{s \in \mathcal{S}} H(s) < \delta$ .
12: return  $O^*(s) = O_i(s), \forall s \in \mathcal{S}_{\text{wait}}, U^*(s) = U_i(s), \forall s \in \mathcal{S}_{\text{comm}}$ .

```

(U), uses the value iteration method of Alg. 2 (see [36]) for a given value of ν ; the *inner decision* is solved in the waiting states with an exhaustive search and in the communication states by the CPSO method described in Sec. V. Note that Alg. 1 references the continuous state and action spaces of the SMDP developed. In practice, the state and action spaces must be discretized in order to numerically evaluate the problem, as is done in the numerical results, Sec. VI.

V. TRAJECTORY OPTIMIZATION VIA CONSTRAINED PARTICLE SWARM OPTIMIZATION

To solve the two-phase *communication* state trajectories when the UAV relays traffic, we must solve $\ell_{\nu}^*(s; U(s))$. However, it involves optimizing over infinitely many variables, $(r_U(t), \theta_U(t))$. To make the optimization tractable, we propose an approximation method based on simplifying the continuous UAV trajectory into a sequence of waypoints connected by straight lines at constant speed; these waypoints and speeds are then optimized using a constrained particle swarm optimization (CPSO) technique. In Sec. VI, we demonstrate that CPSO attains comparable solution accuracy with respect to SCA and up to $100\times$ faster computational speed. The SCA approach has been used in literature to solve non-convex problems [3]; our SCA formulation follows [8], but requires a final end *radius* constraint in place of an end coordinate constraint.

A. Formulation of the Meta-Heuristic UAV Trajectory

To define the UAV meta-heuristic trajectory, we use Cartesian coordinates instead of polar coordinates, since this allows the data payload constraints to be written in closed-form. For

a state $s = (r_U, r, \psi) \in \mathcal{S}_{\text{comm}}$ and a *next radius position* $U(s) = \hat{r}_U$, we define a meta-heuristic trajectory of $\mathbf{q}_U(t)$ by a sequence of M waypoints, $\{\mathbf{x}_m\}_{m=0}^M = \{(x_m, y_m)\}_{m=0}^M$. The UAV trajectory begins at \mathbf{x}_0 and ends at \mathbf{x}_M ; each straight trajectory segment $\Psi_m \triangleq \mathbf{x}_{m+1} - \mathbf{x}_m$ is traversed by a speed $v_m \in [V_{\text{low}}, V_{\text{max}}]$; the sequences $\{\mathbf{x}_m\}_{m=0}^M$ and $\{v_m\}_{m=0}^{M-1}$ are the optimization variables; the sequence of time durations for each trajectory segment is $\{t_m \triangleq \|\Psi_m\|_2/v_m\}_{m=0}^{M-1}$. The maximum speed constraint V_{max} inherited from the original problem (35); however, a minimum speed $V_{\text{low}} \ll V_{\text{max}}$ is introduced so that the durations t_m of each trajectory segment are well-defined. For M trajectory segments, the first $M/2$ and second $M/2$ segments correspond to the two phases of the DF protocol. Finally, because the communication rate equations are angular-invariant, the initial UAV location is set to $\mathbf{x}_0 = (r_U, 0)$ and the GN request location to $\mathbf{x}_G = (x_G, y_G) \triangleq (r \cos \psi, r \sin \psi)$, without affecting the optimization problem.

For each straight trajectory segment, a closed-form solution for the data payload constraints can be obtained, as shown in Lemma 2.

Lemma 2. *The total number of bits transmitted during the m -th trajectory segment, with the UAV starting in position \mathbf{x}_m , ending in position \mathbf{x}_{m+1} , flying at constant speed v_m , is given by*

$$\int_0^{t_m} R_m(d_m(t)) dt = B \cdot (F_m(t_m + \tau_{lb,m}) - F_m(\tau_{lb,m})), \quad (38)$$

where the communication rate during the m th trajectory segment $R_m(d_m(t))$, the distance to transmitter/receiver $d_m(t)$, $\tau_{lb,m}$, and the antiderivative $F_m(\cdot)$ with integration constant 0, are defined in (50), (53), and (54), respectively, found in Appx. A.

With the communication rate integral evaluated, we present the heuristic problem of $\ell_\nu^*(s; U(s))$ to be solved with CPSO. Denoting the trajectory waypoints as $\mathbf{p} \triangleq [\mathbf{x}_1, \dots, \mathbf{x}_{M-1}]^T$ and the segment speeds as $\mathbf{v} \triangleq [v_0, \dots, v_{M-1}]^T$, we write the problem in standard form as

$$(\mathbf{P.0}) \quad \min_{\mathbf{p}, \mathbf{v} \in [V_{\text{low}}, V_{\text{max}}]^M} (1 - \nu P_{\text{avg}}) \sum_{m=0}^{M-1} \frac{\|\Psi_m\|_2}{v_m} + \nu \sum_{m=0}^{M-1} \frac{\|\Psi_m\|_2}{v_m} P_{\text{mob}}(v_m) \quad (39)$$

$$\text{s.t. } h_i(\mathbf{p}, \mathbf{v}) \triangleq L - \sum_{m=\frac{M}{2}(i-1)}^{\frac{M}{2}(i-1)+\frac{M}{2}-1} B \cdot (F_m(t_m + \tau_{lb,m}) - F_m(\tau_{lb,m})) \leq 0, \quad i = 1, 2 \quad (40)$$

$$\mathbf{x}_0 = (r_U, 0), \quad \mathbf{x}_M = \hat{r}_U \cdot \hat{\mathbf{x}}_{M-1}, \quad (41)$$

where $\hat{\mathbf{x}}_{M-1} \triangleq \frac{\mathbf{x}_{M-1}}{\|\mathbf{x}_{M-1}\|_2} \cdot \mathbb{I}(\|\mathbf{x}_{M-1}\|_2 \neq 0) + (1, 0) \cdot \mathbb{I}(\|\mathbf{x}_{M-1}\|_2 = 0)$ ensures that the end radius

constraint is satisfied by projecting the waypoint \mathbf{x}_{M-1} to the nearest point on the radius \hat{r}_U . Thus, the final waypoint variable \mathbf{x}_M can be eliminated, and \mathbf{x}_0 can be fixed. In relation to the original minimization $\ell_\nu^*(s; U(s))$ in (35), the problem (39) is a meta-heuristic approximation. Precisely, (40) are the data payload constraints, $\mathbf{v} \in [V_{\text{low}}, V_{\text{max}}]^M$ are the UAV speed constraints, and (41) gives the initial and end position constraints.

B. Solution of (P.0) via the CPSO Method

As introduced in Sec. I, we solve (P.0) with CPSO, as it promises to provide results efficiently and retain closed-form integrals for the data payload constraints, contrasting discretization and approximation of the SCA constraints. The CPSO method is executed by converting the constrained problem (P.0) into an *unconstrained* one. We remove the data payload constraints by introducing them as additive terms in the objective function to penalize constraint violations by enforcing a particular solution: if the UAV does not receive (or transmit) its data payload at the end of either phase, then it must hover at the current position until it receives (or transmits) the data payload. This penalized objective function is

$$\begin{aligned} \hat{f}(\mathbf{p}, \mathbf{v}) \triangleq & (1 - \nu P_{\text{avg}}) \sum_{m=0}^{M-1} \frac{\|\Psi_m\|_2}{v_m} + \nu \sum_{m=0}^{M-1} \frac{\|\Psi_m\|_2}{v_m} P_{\text{mob}}(v_m) \\ & + (1 - \nu P_{\text{avg}})(\hat{t}_{P,1} + \hat{t}_{P,2}) + \nu(\hat{E}_{P,1} + \hat{E}_{P,2}), \end{aligned} \quad (42)$$

where the time delay penalties for hovering in the first and second phases, respectively, are

$$\hat{t}_{P,1} \triangleq h_1(\mathbf{p}, \mathbf{v})/R_{GU}(\|\mathbf{x}_{M/2} - \mathbf{x}_G\|_2) \cdot \mathbb{I}(h_1(\mathbf{p}, \mathbf{v}) > 0), \quad (43)$$

$$\hat{t}_{P,2} \triangleq h_2(\mathbf{p}, \mathbf{v})/R_{UB}(\|\mathbf{x}_M\|_2) \cdot \mathbb{I}(h_2(\mathbf{p}, \mathbf{v}) > 0), \quad (44)$$

and energy penalties for the UAV hovering in the two phases, respectively, are $\hat{E}_{P,1} \triangleq \hat{t}_{P,1} P_{\text{mob}}(0)$ and $\hat{E}_{P,2} \triangleq \hat{t}_{P,2} P_{\text{mob}}(0)$.

To solve the problem with CPSO, we initialize a population (swarm) of solutions (particles), as well as particle velocity vectors used to update each particle between iterations, using a combination of individual particle history, the swarm history, and randomness. Specifically, we initialize N trajectory waypoint particles $\mathbf{p}_1, \dots, \mathbf{p}_N$ with corresponding particle velocities $\mathbf{u}_1, \dots, \mathbf{u}_N$ and N UAV speed particles $\mathbf{v}_1, \dots, \mathbf{v}_N$ with corresponding particle velocities $\mathbf{w}_1, \dots, \mathbf{w}_N$. The

particles are updated between the k and $(k + 1)$ th iterations by (see [24])

$$\mathbf{p}_i^{k+1} = \mathbf{p}_i^k + \mathbf{u}_i^{k+1}, \quad \mathbf{v}_i^{k+1} = [\mathbf{v}_i^k + \mathbf{w}_i^{k+1}]^{[V_{\text{low}}, V_{\text{max}}]}, \quad (45)$$

where $[\beta]^{[V_{\text{low}}, V_{\text{max}}]}$ is the projection of β to the set $[V_{\text{low}}, V_{\text{max}}]$, which guarantees speed constraints are satisfied at each iteration; the particle velocities are updated according to

$$\mathbf{u}_i^{k+1} = \sigma \left[\mathbf{u}_i^k + c_1 \zeta_i^k (\mathbf{p}_i^{\text{best},k} - \mathbf{p}_i^k) + c_2 \rho_i^k (\mathbf{p}_{\text{swarm}}^{\text{best},k} - \mathbf{p}_i^k) \right], \quad (46)$$

$$\mathbf{w}_i^{k+1} = \sigma \left[\mathbf{w}_i^k + c_1 \zeta_i^k (\mathbf{v}_i^{\text{best},k} - \mathbf{v}_i^k) + c_2 \rho_i^k (\mathbf{v}_{\text{swarm}}^{\text{best},k} - \mathbf{v}_i^k) \right], \quad (47)$$

where c_1 , c_2 , and σ are the cognitive, social, and constriction scaling factors [37], respectively. As [37], [38] point out, $c_1=c_2=2.05$ and $\sigma=0.729$ are common choices for a variety of problems, and we will use these parameters in our upcoming simulations. Additionally, ζ_i^k and ρ_i^k are independent and identically distributed uniform random variables on the interval $[0, 1]$, promoting a degree of random search space exploration. Finally, we define

$$[\mathbf{p}_i^{\text{best},k}, \mathbf{v}_i^{\text{best},k}] = [\mathbf{p}_i^{j^*}, \mathbf{v}_i^{j^*}] \text{ where } j^* \triangleq \arg \min_{0 \leq j \leq k} \{\hat{f}(\mathbf{p}_i^j, \mathbf{v}_i^j)\}, \quad (48)$$

$$[\mathbf{p}_{\text{swarm}}^{\text{best},k}, \mathbf{v}_{\text{swarm}}^{\text{best},k}] = [\mathbf{p}_{i^*}^k, \mathbf{v}_{i^*}^k] \text{ where } i^* \triangleq \arg \min_{1 \leq i \leq N} \{\hat{f}(\mathbf{p}_i^k, \mathbf{v}_i^k)\}, \quad (49)$$

as the currently best position of particle i and currently best position of the swarm at iteration k , respectively [24]. Note that these best particles can be computed in an online fashion as in Algorithm 3. Using the two vectors in (48)–(49) in the particle updates of (45), with the randomness induced by ζ_i^k and ρ_i^k , ensures that subsequent iterations combine knowledge of their personal and the swarm's best solutions, while also exploring to prevent local minima traps. Thus, the CPSO algorithm is given, as in [24], [37], by Alg. 3.

Algorithm 3 CPSO Algorithm for (P.0)

- 1: Randomly initialize \mathbf{p}_i^0 , \mathbf{v}_i^0 , \mathbf{u}_i^0 , and \mathbf{w}_i^0 for all $i = 1, \dots, N$. Set $k = 0$.
- 2: Initialize $[\mathbf{p}_i^{\text{best},0}, \mathbf{v}_i^{\text{best},0}] \leftarrow [\mathbf{p}_i^0, \mathbf{v}_i^0]$ and $[\mathbf{p}_{\text{swarm}}^{\text{best},0}, \mathbf{v}_{\text{swarm}}^{\text{best},0}] \leftarrow \arg \min_{\mathbf{p}_i^0, \mathbf{v}_i^0} \{\hat{f}(\mathbf{p}_i^0, \mathbf{v}_i^0)\}, \forall i$.
- 3: **repeat**
- 4: Update \mathbf{p}_i^{k+1} , \mathbf{v}_i^{k+1} , \mathbf{u}_i^{k+1} , and \mathbf{w}_i^{k+1} according to (45)–(47), respectively, $\forall i$.
- 5: If $\hat{f}(\mathbf{p}_i^{k+1}, \mathbf{v}_i^{k+1}) < \hat{f}(\mathbf{p}_i^{\text{best},k}, \mathbf{v}_i^{\text{best},k})$, then $[\mathbf{p}_i^{\text{best},k+1}, \mathbf{v}_i^{\text{best},k+1}] \leftarrow [\mathbf{p}_i^{k+1}, \mathbf{v}_i^{k+1}]$;
- otherwise, $[\mathbf{p}_i^{\text{best},k+1}, \mathbf{v}_i^{\text{best},k+1}] \leftarrow [\mathbf{p}_i^{\text{best},k}, \mathbf{v}_i^{\text{best},k}]$.
- 6: Update $[\mathbf{p}_{\text{swarm}}^{\text{best},k+1}, \mathbf{v}_{\text{swarm}}^{\text{best},k+1}]$ according to (49).
- 7: $k \leftarrow k + 1$.
- 8: **until** $|\hat{f}(\mathbf{p}_{\text{swarm}}^{\text{best},k}, \mathbf{v}_{\text{swarm}}^{\text{best},k}) - \hat{f}(\mathbf{p}_{\text{swarm}}^{\text{best},k-1}, \mathbf{v}_{\text{swarm}}^{\text{best},k-1})| < \epsilon$.

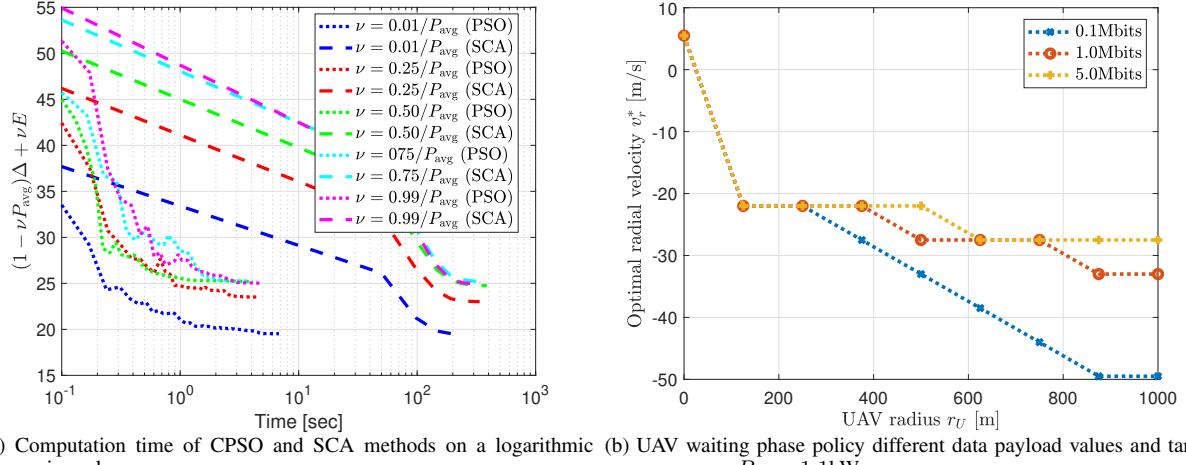
VI. NUMERICAL RESULTS

For the simulation, we use a channel bandwidth of $B=1\text{MHz}$, 1-meter reference SNRs $\gamma_{GB}=\gamma_{GU}=\gamma_{UB}=40\text{dB}$, pathloss exponent $\alpha=2$ for the GN \rightarrow BS link,⁶ UAV height $H_U=120\text{m}$, BS antenna height $H_B=60\text{m}$, maximum UAV speed $V_{\max}=55\text{m/s}$, cell radius $a=1000\text{m}$, and total Poisson rate $\Lambda=0.0085$ req/sec. For the power consumption model, we utilize the relationship given in (3) and the parameters in [8]. We solve an approximation of problem (33) by discretizing the state and action spaces and applying linearly-interpolated value iteration. Additionally, the dual variable ν yields meaningful results in the range $[0, 1/P_{\text{avg}}]$, thus by solving the problem for 20 ν values on the interval, an approximation to the maximum value $g(\nu^*)$ emerges. We discretize the states with $N=9$ equispaced radii values, a single GN in the center of the cell, $K=3$ equispaced angular GN positions in the next radius, $2K$ in the next, and so on, until the N th radius, so that the GN distribution approximates the uniform circular distribution. We discretize $R=21$ equispaced *radial velocity* actions, $v_r \in \{-V_{\max}, \dots, 0, \dots, V_{\max}\}$. For the *next radius position* actions, we use the same radii indexed by the set $\{1, 2, \dots, N\}$. Lastly, Δ_0 is chosen to satisfy $e^{-\Lambda\Delta_0}=0.93$, so that it is unlikely to receive two or more requests in Δ_0 seconds.

A. Comparison of CPSO and SCA Optimization Schemes

To compare CPSO to SCA for solving the inner trajectory optimization, $\ell_{\nu}^*(s; U(s))$, we select a state $s=(800, 500, \pi/4)[\text{m}, \text{m}, \text{rad}]$, end radius $U(s)=700\text{m}$, target average power $P_{\text{avg}}=1.1\text{kW}$, and data payload 1Mbits. For the CPSO approach, we utilize $M_{\text{CPSO}}=4$ line segments (2 for each phase), generate an initial population size of $N_{\text{CPSO}}=75$, and run 7 independent trials of Algorithm 3. Whereas SCA approximates the value of the communication rate integral in each trajectory segment [8], our CPSO formulation evaluates this integral in closed-form (see Lemma 2); thus for the SCA approach, we utilize $M_{\text{SCA}}=100$ trajectory line segments, i.e., a finer discretization, in order to compensate the discretization error. In Fig. 2a, we observe that CPSO performs very competitively with SCA in terms of accuracy, and the CPSO trials converge up to $100\times$ faster in time. Thus, CPSO is preferable in terms of time efficiency, considering that the SMDP discretization results in 981 separate problems to be solved for a fixed ν and P_{avg} .

⁶Note that $\gamma_{GB} = \gamma_{GU} = \gamma_{UB}$ and $\alpha = 2$ are generous, i.e., GN \rightarrow BS channel conditions are as good as the GN \rightarrow UAV and UAV \rightarrow BS links. In less favorable conditions, using the UAV as a relay becomes even more attractive than shown in our numerical evaluations.



(a) Computation time of CPSO and SCA methods on a logarithmic time-axis scale.
(b) UAV waiting phase policy different data payload values and target average power $P_{\text{avg}}=1.1\text{kW}$.

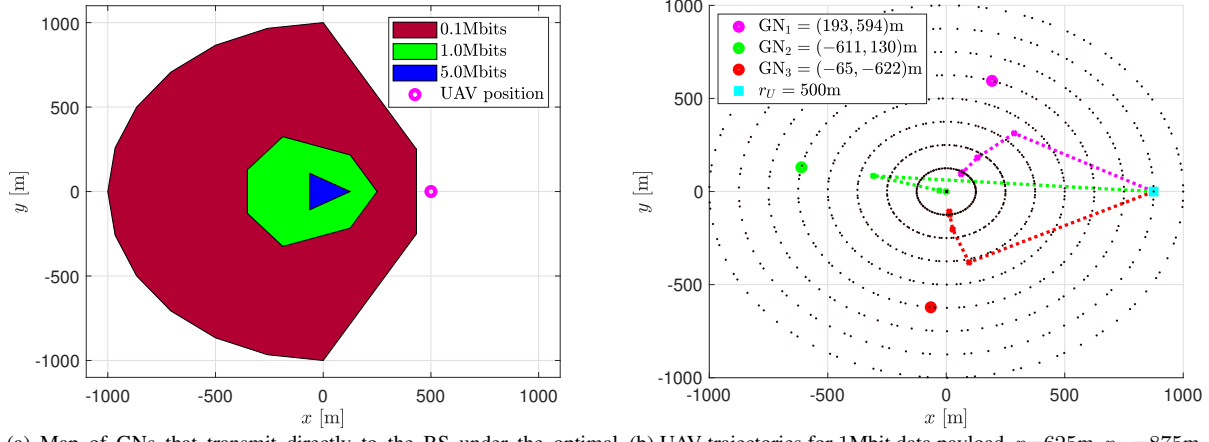
Fig. 2: CPSO/SCA comparison (a) and optimal UAV waiting phase trajectory policy (b).

B. Optimal Policy Structure

To observe the optimal *waiting* phase behavior, we fix $P_{\text{avg}}=1.1\text{kW}$ and vary the data payload values. Fig. 2b demonstrates that the UAV moves toward an optimal flying radius (distance $\leq 125\text{m}$ from the center) during *waiting* phases to address two considerations: 1) to be well-positioned in anticipation of future transmission requests; 2) to fly at the power-minimizing speed in order to reduce UAV energy consumption. Near the cell edge, the UAV radial speed increases for decreasing data payload, as transmission requests with smaller data packets that relay through the UAV take less time to complete transmission than larger ones, thus the UAV is less likely to spend time following trajectories that place it near the cell edge and can afford the additional power consumption required to fly at high speeds when this is the case.

Fig. 3a shows which GNs transmit directly to the BS under the optimal policy $\tilde{\mu}$ during the *communication* phases. The target average power is $P_{\text{avg}}=1.4\text{kW}$, and the UAV radius is fixed to $r_U=500\text{m}$. Most GNs transmit directly to the BS for small data payloads, e.g., 0.1Mbits. As the data payload grows large (1.0 and 5.0Mbits), the benefit of relaying through the UAV and utilizing its mobility increases, so that the majority of GNs relay through the UAV.

Next, we observe the UAV trajectory in *communication* phases across several realizations. In Fig. 3b, we fix the target average power $P_{\text{avg}}=1.4\text{kW}$, initial UAV radius $r_U=875\text{m}$, GN transmission request radius $r=625\text{m}$, and data payload value 1Mbits, and show the optimal trajectories for various UAV-GN angles. In all scenarios, the UAV maintains an approximately constant speed near $V_{\text{max}}=55\text{m/s}$. From the initial position, the UAV does not fly directly toward



(a) Map of GNs that transmit directly to the BS under the optimal policy for $P_{\text{avg}} = 1.4 \text{ kW}$. (b) UAV trajectories for 1Mbit data payload, $r = 625 \text{ m}$, $r_U = 875 \text{ m}$, and $P_{\text{avg}} = 1.4 \text{ kW}$.

Fig. 3: Optimal UAV waiting phase trajectory (a) and communication strategy (b).

the GN of interest, as the trajectory considers both phases of two-phase DF protocol. For the various GN positions, the target end radius of the UAV is selected to be close to the center of the cell, i.e., $\hat{r}_U \leq 125 \text{ m}$, to minimize the long-term delay-power tradeoff.

C. Optimal Performance

To analyze the communication delay performance, we simulate over various data payloads and target average power constraints, P_{avg} , to observe a range of behavior. The expected average delay is shown in Figs. 4a–4c. Note that the expected average delay, $\bar{D}_{\tilde{\mu}}$, is not directly accessible through the value iteration analysis, so we apply the optimal policy $\tilde{\mu}$ in a simulation, sampling a sequence of several thousand random transmission requests, in order to obtain it. Using the transmission request sequence, we compare $\bar{D}_{\tilde{\mu}}$ against *four* heuristics, explained as follows:

- (1) *UAV only*: all actions remain the same, except GNs may not directly transmit to the BS
- (2) *Direct to BS*: no UAV is deployed; all GNs transmit directly to the BS⁷.
- (3) *Static UAV*: the UAV hovers at the optimized radius $r_U^* = 321.61 \text{ m}$; GN transmission requests may directly transmit to the BS or relay through the UAV so as to minimize delay.
- (4) *Greedy*: scheduling decisions greedily minimize the delay incurred to serve transmission requests; if the UAV is chosen for relaying, it executes a trajectory to minimize the communication delay; the UAV hovers statically after communication phases until receiving a new request.

⁷Note that the UAV consumes 0W in this policy, but the data points in Figs. 4a–4c are at $P_{\text{avg}} = 1.1 \text{ kW}$ to fit in the axes.

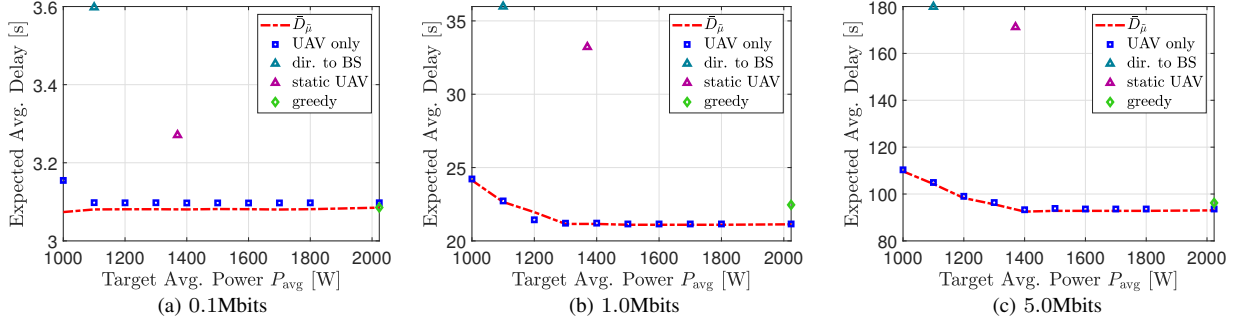


Fig. 4: Expected average communication delay vs. P_{avg} for optimal policy $\tilde{\mu}$, various heuristics, and continuous-space simulation.

Across the range of data payloads and target average powers, the optimal policy simulation reduces the average communication delay by up to 49% when compared to the *direct to BS* heuristic. The UAV consumes 1.37kW to hover following the *static UAV* scheme, and when compared to the optimal policy with $P_{avg}=1.3$ kW, the UAV consumes 1.02, 1.26, and 1.28kW for the 0.1, 1.0, 5.0Mbits data payloads, respectively, while reducing the average communication delay by 6%, 36%, and 44%, respectively, thus showing that optimally exploiting UAV mobility can simultaneously reduce communication delay and power consumption. Next, the optimal policy slightly reduces the communication delay (up to 3%) with respect to the *UAV only* heuristic, which does not adaptively schedule transmission requests but still exploits UAV mobility. The UAV power consumption is unconstrained in the *greedy* heuristic, but fails to exploit UAV mobility for long-term goals. For example, in the 1.0Mbits case (Fig. 4b), the UAV consumes 1.58kW on average for mobility following the *greedy* scheme, yet the optimal strategy reduces both communication delay and power consumption for target average powers $P_{avg} \geq 1.2$ kW. When $P_{avg}=1.2$ kW, for instance, the optimal strategy reduces the average communication delay and UAV mobility power by 2% and 13%, respectively.

VII. CONCLUSIONS

In this paper, we studied the adaptive trajectory and communication scheduling design of a power-constrained UAV serving as a relay for random data traffic between GNs and a BS. The problem was cast as a SMDP, and we showed that it exhibits a two-scale structure that can be efficiently optimized. Overall, we showed that by optimally exploiting realistic features of UAV mobility and adaptively scheduling transmission requests, both the expected average communication delay and UAV mobility power consumption can be reduced when compared to an optimal hovering deployment and a greedy delay minimization scheme.

APPENDIX A

EVALUATION OF DATA PAYLOAD INTEGRALS FOR DISCRETIZED TRAJECTORY SEGMENTS

For an initial UAV position \mathbf{x}_m at time $t = 0$, flying to \mathbf{x}_{m+1} at speed v_m for t_m seconds, the communication rate integral is

$$\int_0^{t_m} R_m(d_m(t))dt \triangleq \int_0^{t_m} B \cdot \log_2 \left(1 + \frac{\gamma_m}{H_m^2 + (a_m t + c_m)^2 + (b_m t + g_m)^2} \right) dt, \quad (50)$$

where $d_m(t) = \sqrt{H_m^2 + (a_m t + c_m)^2 + (b_m t + g_m)^2}$ is the distance between transmitter and receiver at time t , $a_m = v_m \cdot (x_{m+1} - x_m) / \|\Psi_m\|_2$, $b_m = v_m \cdot (y_{m+1} - y_m) / \|\Psi_m\|_2$, and

$$\begin{cases} \gamma_m = \gamma_{GU}, H_m = H_U, c_m = x_m - x_{GN}, g_m = y_m - y_{GN}, \forall m \in \{0, \dots, M/2 - 1\}, \\ \gamma_m = \gamma_{UB}, H_m = H_U - H_B, c_m = x_m, g_m = y_m, \forall m \in \{M/2, \dots, M - 1\}. \end{cases} \quad (51)$$

To evaluate (50), we first rewrite it as

$$\int_{\tau_{lb,m}}^{t_m + \tau_{lb,m}} B \cdot \log_2 \left(1 + \frac{\gamma_m}{A_{1,m} + A_{2,m}\tau^2} \right) d\tau = B \cdot (F_m(t_m + \tau_{lb,m}) - F_m(\tau_{lb,m})), \quad (52)$$

as (52) has a simple, closed-form solution [7]. With variable substitution, we get the following equivalent parameters

$$A_{1,m} = H_m^2 - \tau_{lb,m}^2 A_{2,m} + c_m^2 + g_m^2, \quad A_{2,m} = a_m^2 + b_m^2, \quad \tau_{lb,m} = \frac{a_m c_m + b_m g_m}{a_m^2 + b_m^2}, \quad (53)$$

where the antiderivative with integration constant 0 is

$$\begin{aligned} F_m(u) \triangleq u \log_2 \left(1 + \frac{\gamma_m}{A_{1,m} + A_{2,m}u^2} \right) + \frac{2\sqrt{\gamma_m + A_{1,m}} \tan^{-1} \left(\frac{\sqrt{A_{2,m}}u}{\sqrt{\gamma_m + A_{1,m}}} \right)}{\sqrt{A_{2,m}} \ln(2)} \\ - \frac{2\sqrt{A_{1,m}} \tan^{-1} \left(\frac{\sqrt{A_{2,m}}u}{\sqrt{A_{1,m}}} \right)}{\sqrt{A_{2,m}} \ln(2)}. \end{aligned} \quad (54)$$

REFERENCES

- [1] M. Bliss and N. Michelusi, "Power-constrained trajectory optimization for wireless uav relays with random requests," 2019. To appear at IEEE ICC 2020, pp. 1–6.
- [2] A. Fotouhi, H. Qiang, M. Ding, M. Hassan, L. G. Giordano, A. Garcia-Rodriguez, and J. Yuan, "Survey on uav cellular communications: Practical aspects, standardization advancements, regulation, and security challenges," *IEEE Communications Surveys Tutorials*, pp. 1–1, 2019.

- [3] M. Mozaffari, W. Saad, M. Bennis, Y. Nam, and M. Debbah, "A tutorial on uavs for wireless networks: Applications, challenges, and open problems," *IEEE Communications Surveys Tutorials*, pp. 1–1, 2019.
- [4] L. Gupta, R. Jain, and G. Vaszkun, "Survey of important issues in uav communication networks," *IEEE Communications Surveys Tutorials*, vol. 18, no. 2, pp. 1123–1152, Secondquarter 2016.
- [5] Y. Zeng, R. Zhang, and T. J. Lim, "Wireless communications with unmanned aerial vehicles: opportunities and challenges," *IEEE Communications Magazine*, vol. 54, no. 5, pp. 36–42, May 2016.
- [6] Q. Wu, L. Liu, and R. Zhang, "Fundamental Trade-offs in Communication and Trajectory Design for UAV-Enabled Wireless Network," *IEEE Wireless Communications*, vol. 26, pp. 36–44, 02 2019.
- [7] Y. Zeng and R. Zhang, "Energy-efficient uav communication with trajectory optimization," *IEEE Transactions on Wireless Communications*, vol. 16, no. 6, pp. 3747–3760, June 2017.
- [8] Y. Zeng, J. Xu, and R. Zhang, "Energy Minimization for Wireless Communication With Rotary-Wing UAV," *IEEE Transactions on Wireless Communications*, vol. 18, no. 4, pp. 2329–2345, April 2019.
- [9] M. Mozaffari, W. Saad, M. Bennis, and M. Debbah, "Optimal transport theory for power-efficient deployment of unmanned aerial vehicles," in *2016 IEEE International Conference on Communications (ICC)*, May 2016, pp. 1–6.
- [10] S. Zhang, Y. Zeng, and R. Zhang, "Cellular-enabled uav communication: A connectivity-constrained trajectory optimization perspective," *IEEE Transactions on Communications*, vol. 67, no. 3, pp. 2580–2604, March 2019.
- [11] F. Jiang and A. L. Swindlehurst, "Optimization of uav heading for the ground-to-air uplink," *IEEE Journal on Selected Areas in Communications*, vol. 30, no. 5, pp. 993–1005, June 2012.
- [12] S. ur Rahman, G. Kim, Y. Cho, and A. Khan, "Positioning of uavs for throughput maximization in software-defined disaster area uav communication networks," *Journal of Communications and Networks*, vol. 20, no. 5, pp. 452–463, 2018.
- [13] O. Esrafilian, R. Gangula, and D. Gesbert, "Uav-relay placement with unknown user locations and channel parameters," in *2018 52nd Asilomar Conference on Signals, Systems, and Computers*, 2018, pp. 1075–1079.
- [14] X. Li, D. Guo, H. Yin, and G. Wei, "Drone-assisted public safety wireless broadband network," in *2015 IEEE Wireless Communications and Networking Conference Workshops (WCNCW)*, 2015, pp. 323–328.
- [15] A. Fotouhi, M. Ding, and M. Hassan, "Dynamic base station repositioning to improve performance of drone small cells," in *2016 IEEE Globecom Workshops (GC Wkshps)*, Dec 2016, pp. 1–6.
- [16] Y. Chen, N. Zhao, Z. Ding, and M. Alouini, "Multiple uavs as relays: Multi-hop single link versus multiple dual-hop links," *IEEE Transactions on Wireless Communications*, vol. 17, no. 9, pp. 6348–6359, Sep. 2018.
- [17] A. Al-Hourani, S. Kandeepan, and S. Lardner, "Optimal LAP Altitude for Maximum Coverage," *IEEE Wireless Communications Letters*, vol. 3, no. 6, pp. 569–572, 2014.
- [18] Q. Zhang, M. Mozaffari, W. Saad, M. Bennis, and M. Debbah, "Machine learning for predictive on-demand deployment of uavs for wireless communications," in *2018 IEEE Global Communications Conference (GLOBECOM)*, 2018, pp. 1–6.
- [19] M. Mozaffari, W. Saad, M. Bennis, and M. Debbah, "Mobile unmanned aerial vehicles (uavs) for energy-efficient internet of things communications," *IEEE Transactions on Wireless Communications*, vol. 16, no. 11, pp. 7574–7589, 2017.
- [20] V. Saxena, J. Jaldén, and H. Klessig, "Optimal uav base station trajectories using flow-level models for reinforcement learning," *IEEE Transactions on Cognitive Communications and Networking*, vol. 5, no. 4, pp. 1101–1112, 2019.
- [21] J. Hu, H. Zhang, and L. Song, "Reinforcement learning for decentralized trajectory design in cellular uav networks with sense-and-send protocol," *IEEE Internet of Things Journal*, vol. 6, no. 4, pp. 6177–6189, 2019.
- [22] A. M. Koushik, F. Hu, and S. Kumar, "Deep Q -learning-based node positioning for throughput-optimal communications in dynamic uav swarm network," *IEEE Transactions on Cognitive Communications and Networking*, vol. 5, no. 3, pp. 554–566, 2019.

- [23] W. Johnson, *Rotorcraft aeromechanics*, ser. Cambridge aerospace series ; 36. Cambridge: Cambridge University Press, 2013.
- [24] M. Clerc, *Particle swarm optimization*, ser. ISTE. London ; Newport Beach: ISTE, 2006.
- [25] H. Shakhatreh, A. Khreishah, A. Alsafran, I. Khalil, A. Sawalmeh, and N. S. Othman, “Efficient 3d placement of a uav using particle swarm optimization,” in *2017 8th International Conference on Information and Communication Systems (ICICS)*, 2017, pp. 258–263.
- [26] Z. Yuheng, Z. Liyan, and L. Chunpeng, “3-d deployment optimization of uavs based on particle swarm algorithm,” in *2019 IEEE 19th International Conference on Communication Technology (ICCT)*, 2019, pp. 954–957.
- [27] J. Cho and J. Kim, “Performance comparison of heuristic algorithms for uav deployment with low power consumption,” in *2018 International Conference on Information and Communication Technology Convergence (ICTC)*, 2018, pp. 1067–1069.
- [28] S. A. Hadiwardoyo, C. T. Calafate, J. Cano, K. Krinkin, D. Klionskiy, E. Hernández-Orallo, and P. Manzoni, “Optimizing uav-to-car communications in 3d environments through dynamic uav positioning,” in *2019 IEEE/ACM 23rd International Symposium on Distributed Simulation and Real Time Applications (DS-RT)*, 2019, pp. 1–8.
- [29] A. H. Kulaç, A. Akarsu, and T. Girici, “Optimal deployment of uav’s for communication,” in *2018 26th Signal Processing and Communications Applications Conference (SIU)*, 2018, pp. 1–4.
- [30] R. K. Patra and P. Muthuchidambaranathan, “Optimisation of spectrum and energy efficiency in uav-enabled mobile relaying using bisection and pso method,” in *2018 3rd International Conference for Convergence in Technology (I2CT)*, 2018, pp. 1–7.
- [31] M.-H. Hwang, H.-R. Cha, and S. Jung, “Practical endurance estimation for minimizing energy consumption of multirotor unmanned aerial vehicles,” *Energies*, vol. 11, no. 9, 2018.
- [32] H. Bayerlein, P. De Kerret, and D. Gesbert, “Trajectory Optimization for Autonomous Flying Base Station via Reinforcement Learning,” in *IEEE 19th International Workshop on Signal Processing Advances in Wireless Communications (SPAWC)*, June 2018, pp. 1–5.
- [33] M. Bliss and N. Michelusi, “Trajectory optimization for rotary-wing uavs in wireless networks with random requests,” in *2019 IEEE Global Communications Conference (GLOBECOM)*, 2019, pp. 1–6.
- [34] J. D. C. Little and S. Graves, *Little’s Law*, 07 2008, pp. 81–100.
- [35] S. Boyd, L. Xiao, and A. Mutapcic, “Subgradient methods,” *lecture notes of EE392o, Stanford University, Autumn Quarter*, vol. 2004, pp. 2004–2005, 2003.
- [36] M. L. Puterman, *Markov decision processes: discrete stochastic dynamic programming*. John Wiley & Sons, 2014.
- [37] T.-H. Kim, I. Maruta, and T. Sugie, “A simple and efficient constrained particle swarm optimization and its application to engineering design problems,” *Proceedings of the Institution of Mechanical Engineers, Part C: Journal of Mechanical Engineering Science*, vol. 224, no. 2, pp. 389–400, 2010.
- [38] I. C. Trelea, “The particle swarm optimization algorithm: convergence analysis and parameter selection,” *Information Processing Letters*, vol. 85, no. 6, pp. 317–325, 2003.